POAC'25
St. John's, Newfoundland and Labrador, Canada

Proceedings of the 28th International Conference on Port and Ocean Engineering under Arctic Conditions
Jul 13-17, 2025
St. John's, Newfoundland and Labrador
Canada

# Evaluating the Structural Response of Light Ice-Class Ships Under Ice Loads

Samaneh Sadeghi[1], Bruce W.T. Quinton[1], Edward Moakler[2], Jennifer Smith[1], Brian Veitch[1]

[1] Faculty of Engineering and Applied Science, Memorial University of Newfoundland, St. John's, NL. Canada

[2] ABS Canada Inc. Ottawa, ON. Canada

## ABSTRACT

In Arctic waters, ship structures are exposed to various forces, including ice impact loads. Assessing structural capabilities is crucial for understanding the hull's capacity and ensuring the safety of vessels, crews, and the environment. The capacity of ship structures represents a limit at which vessels can be operated without surpassing safe boundaries, thereby avoiding damage. This paper demonstrates a methodology for characterizing the structural responses to a range of ice load magnitudes for the purposes of providing feedback to mariners. The approach uses the bow grillage panel of a low Polar Class ship as an example in compliance with the International Association of Classification Societies Polar Class rules. The ice-crushing forces are estimated using a combination of the Popov model and the pressure-area curves method for the specified light ice conditions and ship-ice contact geometry. Then, the behavior of the hull is examined by applying the design load and a progressive series of ice loads to the middle of the panel. Finite Element Analysis is implemented to develop a look-up table outlining the structural response for each ice force and demonstrating limits corresponding to the structure's design and repair-required levels. The look-up table enables a comparison to thresholds corresponding to the structure's design and repair-required limits. The practical implications of this study are intended to provide advice for ship operators to enhance the safety of light Polar Class ship structures when navigating in ice-covered waters.

KEY WORDS: Ice-class ships; Structural response; Ice load; Polar class; Collisions.

## INTRODUCTION

When vessels are navigating in ice-covered waters, the structure is exposed to different forces, including ice impact loads. The interaction between a vessel and sea ice is a complex process, influenced by various factors, including the ice conditions, the geometric characteristics of the ship's hull, and the relative velocity between the vessel and the ice (Lubbad & Løset, 2011). Consequently, ice navigators should possess comprehensive knowledge of ice characteristics and operational instructions conducive to a safe voyage (Canadian Coast Guard, 2022). Thus, to operate safely in Arctic waters, those operating the vessel must understand a ship's structural capabilities under a range of ice loads. The capacity of ship structures represents a limit at which vessels can be operated without surpassing safe boundaries, thereby avoiding damage. This paper presents a methodology for characterizing the structural responses to a range of ice load magnitudes.

The methodology models ship-ice collision using a combination of the Popov model and the pressure-area curves method (Popov et al., 1969; Daley, 1999).

Ship-ice interaction has to be investigated to model the impact and facilitate the enhancement of the design and operation of vessels navigating through the ice (Lubbad & Løset, 2011). Previous research has been conducted on ship collisions and grounding in Arctic waters, especially ship-ice interactions and their effects on marine structural capacities (Minorsky, 1958; Popov et al., 1969; Daley & Kim, 2010; Lubbad & Løset, 2011; Ehlers & Tabri, 2012; Quinton, 2015; Zhang et al., 2020). Popov et al.'s model was one of the earliest analytical energy methods to equate the forces resulting from a collision to the amount of dissipating ice crushing. The model simplified the assumptions of the collision from a six-degree of freedom system into a one-dimensional problem. Daley (1999) adapted the Popov method with pressure-area curves to estimate ice-crushing force on a ship hull.

The International Association of Classification Societies (IACS) Polar Class Unified Requirements (UR) provide standardized ice-class rules for ships operating in Polar waters. These rules emphasize a hierarchical structural arrangement, where longitudinal and transverse stiffeners reinforce the ship's shell plating with appropriate frame spacing for specific ice operations (IACS, 2019).

Ice class rules traditionally emphasized the structure's elastic behavior and weak areas were defined as those typically expected to yield or fail first. However, ship structures are capable of withstanding loading conditions well beyond initial yield before collapsing entirely. The grillage, including plates, frames, and stringers, has initial strength and considerable reserve strength. The IACS UR Polar Class rules formulate the combined stress of the structural grillage based on plastic limit states to establish a substantial reserve of strength (Daley et al., 2007). The Finite Element Analysis (FEA) has been widely used to assess ship structural responses due to their demonstrated accuracy in predicting failure criteria and ice load limits, as well as their ability to analyze post-yield behavior under lateral loads (Quinton, 2015).

This work studies the bow grillage panel of a light Polar Class ship as a case study. FEM is used to investigate the structural behavior of the grillage, including elastic and post-yield behaviors under a progressive series of ice loads corresponding to increasing energy levels. The structural response analysis was examined to develop a look-up table outlining the structural response for each ice force corresponding to the structure's design and repair-required levels. The incremental loading levels continued until the failure criteria were satisfied. Two case studies were conducted to demonstrate the methodology.

The ultimate goal of this work is to contribute to future feedback and advisory systems for the ships' bridge through which the operators will have access to and practical understanding of the structural capacities and limitations of the ships they operate.

## METHODOLOGY

### Ship-Ice Interaction Model

In ship-ice interaction, the amount of energy dissipated due to the vessel's motion and ice crushing should be determined to calculate the available energy that leads to structural deformations (Zhang et al., 2020). The ship-ice impact is modeled here using a combination of the Popov-Daley method (Popov et al., 1969; Daley, 1999). The interaction is assumed to be a glancing impact on the shoulder with an ice floe edge and a momentary 'normal' type impact, where the available normal kinetic energy ($KE_n$) is equated to the energy absorbed for crushing the ice (IE), shown in Equation (1). Other forces (friction, damping, and buoyancy effects) are neglected to make the kinetic energy equation solvable. The laws of momentum conservation, energy conservation, and mass conservation must be satisfied.

$$KE_n = IE \quad (1)$$

The normal kinetic energy is calculated using Equation (2), where $M_e$ is the effective collision mass (combining ship and ice floe masses) and $V_n$ is the relative normal velocity of the ship at the point of impact.

$$KE_n = \tfrac{1}{2} M_e V_n^2 \quad (2)$$

The model assumes that the ice force is only related to ice indentation. The force acts normal to the hull at the contact point because there is no friction. When the vessel penetrates the ice, the contact force increases. When this force is maximum at the time of maximum penetration, the $KE_n$ will reach zero. The pressure-area model examined an average pressure for a nominal contact area, which is determined by analyzing the geometric overlap between the ice and structure and the extent of indentation using Equation (3).

$$P_{avg} = P_0 \,.\, A_n^{\,ex} \quad (3)$$

where $P_0$ is the nominal crushing pressure on one square meter of ice and is assumed to be 1.25 MPa, $A_n$ is the nominal crushing area, ex is the empirical ice crushing constant and is assumed to be -0.1, $\zeta$ is the ice crushing depth, and $f_a$ and $f_x$ are form factors. Then, the ice force ($F_n$) is equated as follows due to its relationship with the contact area.

$$A_n = \zeta \,.\, f_a \quad (4)$$

$$F_n = P_{avg} \,.\, A_n = P_0 \,.\, A_n^{\,1+ex} = P_0 \,.\, f_a \,.\, \zeta^{\,f_x -1} \quad (5)$$

The impact geometry affects how the indentation and normal crushing area are related. It is assumed here to be a symmetric general wedge. For this, a wedge angle ($\phi$), which signifies the breadth of the ice wedge involved in the collision, is taken to be $150^0$ (Daley et al., 2017). A normal frame angle ($\beta'$) is assumed to be $47.5^0$.

$$\zeta = (KE \,.\, f_x / P_0 \,.\, f_a)^{1/f_x} \quad (6)$$

$$f_x = 3 + 2\,ex \quad (7)$$

$$f_a = [\,Tan(\phi/2) / (Sin(\beta') \,.\, Cos^2(\beta'))]^{1+ex} \quad (8)$$

**Re-dimensioning of the Structural Grillage**

A typical light Polar Class 7 (PC7) ship was chosen for this work to investigate the structural responses under the increasing ice forces and to develop a corresponding look-up table. The re-dimensioning of scantlings and the structural arrangement were determined using *PC Design & Check*, a program developed by Daley. The IACS UR Polar Class rules have been implemented in this software as a Microsoft® Excel™ program. The minimum scantling designed structures were checked and confirmed with an ABS-developed tool, *ABS Ice Quick Check*. The vessel's structural scantling design parameters are listed in Table 1. The structural grillage consists of two built-T longitudinal stringer spans and supports 14 transverse frames at each span. The grillage particulars are listed in Table 2 and shown in Figure 1. The grillage boundary conditions were fixed at all four sides to avoid any deformations and rotations at those locations in all six degrees of freedom.

Table 1. PC7 Structural scantling design parameters

| Parameter | Value |
|---|---|
| Displacement, Kt | 3.9 |
| Hull Region | Bow |
| Frame Orientation Angle, deg | 90 |
| Frame Orientation Type | Transverse |
| Water Density, kg/m$^3$ | 1025 |
| Frame Attachment Parameters | 2 |
| Main Frame Span, mm | 2000 |
| Main Frame Spacing, mm | 400 |

Table 2. Structural scantling particulars of PC7

| Particular | Dimension (mm) |
|---|---|
| Plate Thickness | 15.5 |
| Frame Scantlings (Flat bars) | 200 x 16 |
| Stringer Scantlings (Built-T) | 400 x 12<br>120 x 8 |

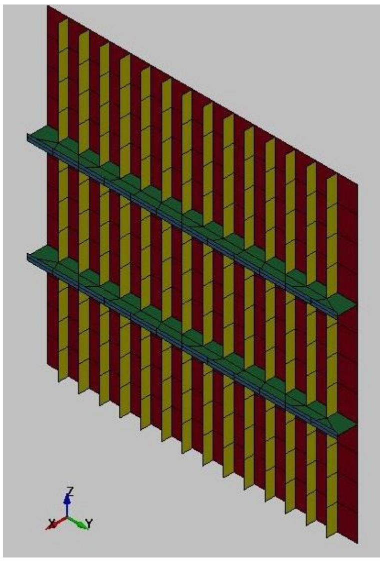


Figure 1. Structural grillage

## NUMERICAL MODEL IN FEA

The two main areas of study for ship impact or collision physics analysis are external and internal mechanics. External mechanics pertain to the rigid body motion of the ship at the time of impact, along with the hydrodynamic pressures exerted over its wetted surface. Internal mechanics encompass the structural response of the ship during impact or collision, including the subsequent deformation (Pedersen, 1995). Internal collision mechanics have been considered in this work regarding the structural response of the shells and frames.

Finite Element Analysis (FEA) was used to investigate the structural response. FEA is typically conducted using commercially available software. One of the primary advantages of the FEA is its ability to effectively analyze larger deformations extending into the plastic region due to loads above the design load, which is not as readily achievable through the Polar Class rules. This capability facilitates the identification of additional structural thresholds beyond the design load (Dolny et al., 2013). The bow grillage panel, 6m (tall) x 6m (wide), was modeled in Rhino3D. The analysis is conducted under the assumption of a flat surface, neglecting curvature effects. This simplification is justified as ice pressure is directly incorporated into the structural response calculations in the FEA and the orientation does not influence. Loads were applied at the center of the panel using LS-Dyna. The geometry was meshed using four-node shell elements based on the Belytschko-Tsay formulation, which incorporated five through-thickness integration points. A convergence analysis, based on the maximum deformation observed at the center of the load patch, indicated that an average mesh size of 25 mm is suitable for the simulation. As an increase in ice loads and pressures leads to greater collision energy and ice penetration, each load application requires a newly defined patch area. This process can be time-consuming. For this study, increasing ice pressures for a fixed-size load patch were applied. The process continued until the failure criteria were met.

A bilinear elastic-plastic material model was chosen. This model assumes a linear stress-strain relationship in both elastic and plastic regions, with different slopes for each segment. In fact, the relationship between stress and strain in plastic areas is non-linear. The elastic-plastic material model in the FEA refers to a material formulation that is nonlinear, allowing the material to undergo both elastic and plastic deformations, as required (Hallquist, 2006). No dynamic loading conditions or time-dependent influences have been incorporated in this model. The material parameters of the panel are shown in Table 3.

Table 3. Material parameters

| **Density ($kg/m^3$)** | **Yong's Modulus (GPa)** | **Yield Strength (MPa)** | **Poisson's Ratio (MPa)** | **Tangent Modulus (MPa)** |
|---|---|---|---|---|
| 7850 | 207 | 315 | 0.3 | 1000 |

In this work, failure criteria were categorized into two thresholds. The first threshold, named the design limit, was based on IACS UR Polar Class rules and defined the design ice load as a uniform average pressure applied to the ship's plating. With significant plastic strength reserves, the frame was designed to endure loads beyond its elastic limit. The design ice force ($F_{Bow}$) and line load ($Q_{Bow}$) for the bow region are calculated according to the IACS UR Polar Class rules for the chosen vessel (IACS, 2019). The results are outlined in Table 4.

Table 4. Design ice force, line load, pressure, and load patch dimensions for the bow region

| **Force (MN)** | **Line load (MN/m)** | **Width (m)** | **Height (m)** | **Average pressure (MPa)** |
|---|---|---|---|---|
| 0.28 | 0.32 | 0.87 | 0.21 | 1.55 |

The second threshold, named the repair limit, occurs when deformation surpasses the design load, necessitating structural repairs as per IACS Recommendation No. 47, Shipbuilding and Repair Quality Standard Rev. 5, dated October 2010. In this reference, structural failure was defined as the point at which any frame undergoes lateral deformation exceeding 25mm × (S/10), where S represents the span in meters. The allowable distortion in the Y-direction for the frames with a stringer spacing of 2,000 mm is 5 mm (IACS, 2010). Loads started with the design ice pressure at 1.55 MPa and increased gradually for the fixed design load patch size.

## RESULTS AND CASE STUDIES

This section presents the FEA results for the bow grillage panel. The structure was subjected to the design ice load. The trial-and-error approach determined that applying a pressure of 6.2 MPa (approximately 2.30 MN force) resulted in permanent lateral deformation in the grillage that closely matched the failure repair criteria. In all cases, the highest deformation was observed on the shell plating in the direction of the applied load patch, the X-direction. The corresponding ice-crushing strength and energy associated with the applied pressure were determined using the provided equations in 2.1. Considering an allowable permanent deformation limit of 5 mm that remains after the load is removed, the corresponding collision energy for the design and repair limits was determined to be approximately 40 KJ and 340 KJ, respectively. Collision energies below the repair limit were regarded as within the conservative operational range. The results are shown in Table 5 and Figure 2. The findings show that structural responses intensify as collision energy levels increase. The grillage failure at the repair threshold is indicated in Figure 3.

Table 5. FEA results

| Ice Pressure (MPa) | Normal Ice Force (MN) | Collision Energy (KJ) | Lateral deformation in transverse frames (mm) | Maximum deformation in shell plating (mm) |
|---|---|---|---|---|
| 1.55 | 0.57 | 39.13 | 0.8 | 6.0 |
| 3.00 | 1.10 | 109.29 | 1.5 | 11.5 |
| 5.00 | 1.83 | 241.92 | 3.0 | 27.0 |
| 6.00 | 2.19 | 321.25 | 4.5 | 38.0 |
| 6.24 | 2.28 | 341.46 | 5.0 | 41.0 |
| 7.50 | 2.74 | 454.57 | 7.0 | 56.5 |
| 15.0 | 5.48 | 1336.18 | 16.0 | 116.0 |

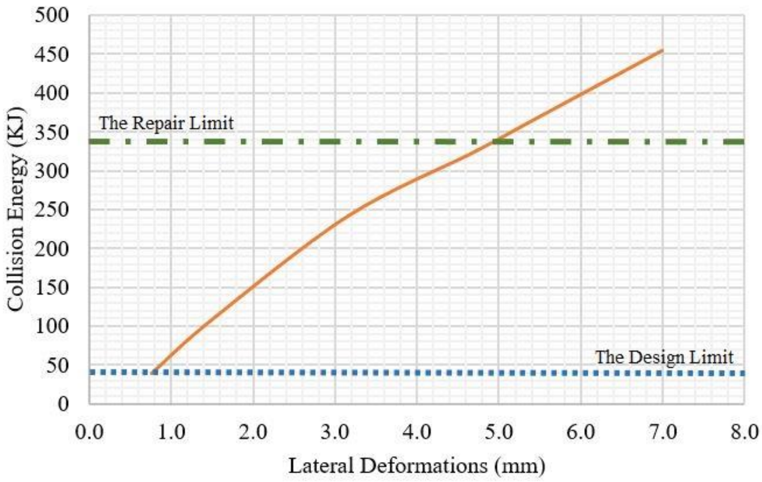


Figure 2. Lateral Deformations for Various Collision Energies

PC7s operate in thin first-year ice fields in summer/autumn (IACS, 2019). Two case studies for different ice conditions were conducted to illustrate how this methodology works and how mariners could benefit from it. It was assumed that the wedge-angle impacts occur in a known location of the bow in coordinates and frame angle.

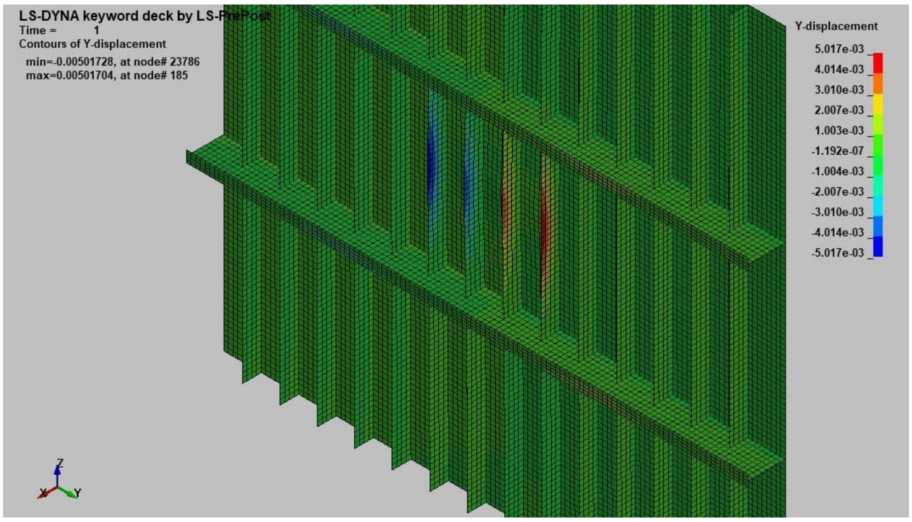

Figure 3. Lateral Deformation of 5 mm

**Case study 1**

This case considered a ship colliding with a 10m square ice floe of some assumed thickness. The assumed ice thicknesses for thin first-year ice (30 cm, 50 cm, and 70 cm). The corresponding ice-collision energy associated with these ice floes for various ship speeds was determined using Equation 2. Results are presented in Figures 4 and 5.

Figure 4 demonstrates that the collision energy magnitudes increase when ship speed and ice thickness increase. Figure 5 shows that the speeds associated with the repair limit deformation (of 5 mm for the structure in this case) increase as ice thickness decreases. The approximate repair-limit speed of the vessel is shown in Table 6.

Table 6. Case 1: Repair-limit speed in different ice thicknesses

| Ice Thickness (cm) | Speed (m/s) |
|---|---|
| 30 | 13 |
| 50 | 10 |
| 70 | 8.5 |

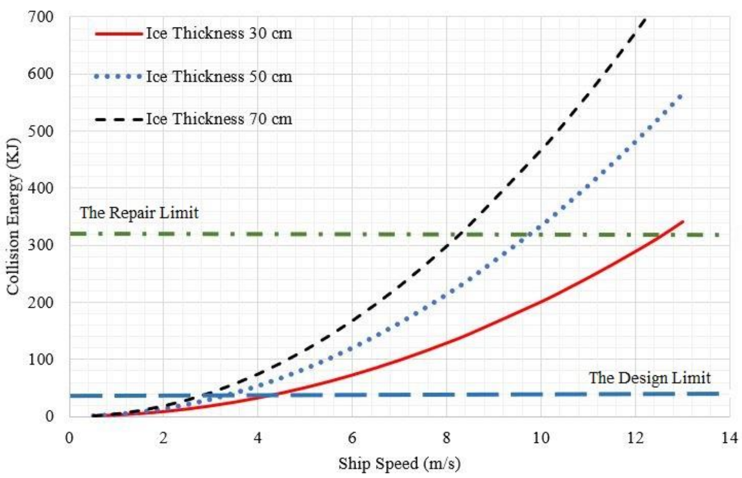

Figure 4. Collision energies for a range of ship speed

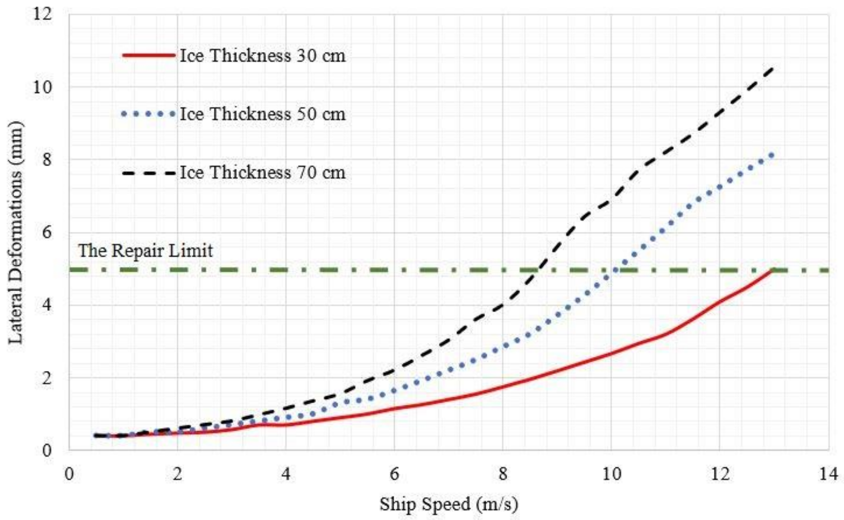


Figure 5. Lateral deformations for a range of ship speed

**Case Study 2**

The second case considered the same ship and structure, this time colliding with a smaller floe (10 m x 5 m) with a thickness of 50 cm. The impact sketch is shown in Figure 6. The corresponding ice-collision energy for various ship speeds was calculated.

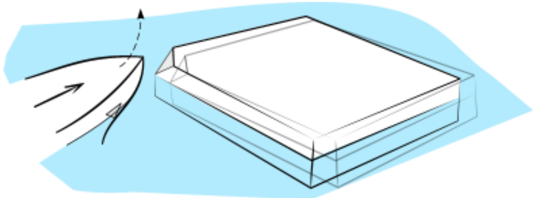

Figure 6. Finite Ice Floe (Daley et al., 2017)

Figures 7 and 8 show that the collision energy magnitudes increase when the ship speed increases for this case. The ship speed at the collision energy associated with the repair limit of deformation (5 mm as before) was found to be 13.5 m/s.

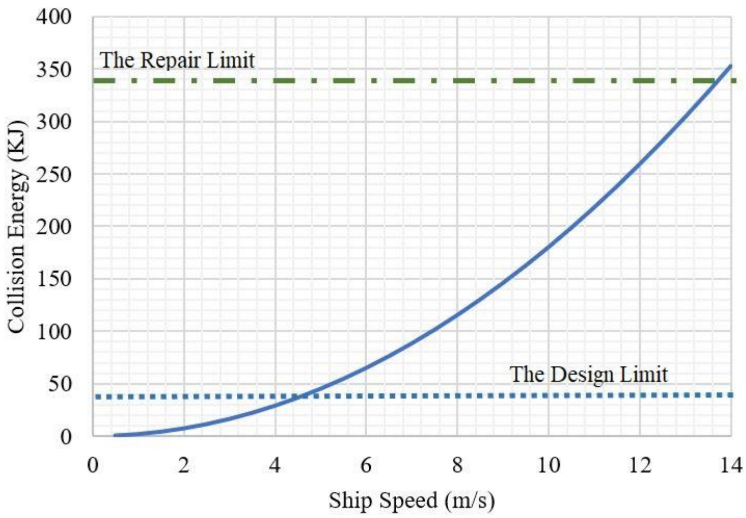


Figure 7. Collision energies for a range of ship speed

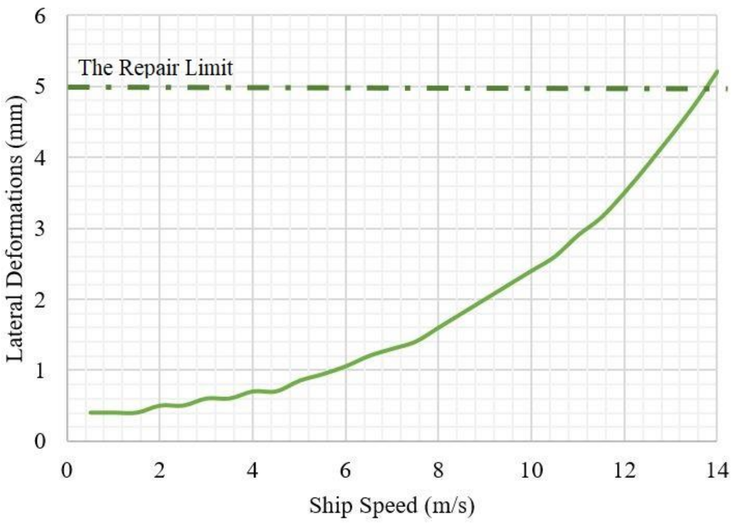


Figure 8. Lateral deformations for a range of ship speeds

## CONCLUSIONS

The FEA simulations provide insights into ship frames' plastic behavior and reserve capacity under a range of ice loads. The look-up table (Table 5) provides further information on the relationships between collision energy and structural response.

It is important to highlight that the methodology presented in this study is sensitive to the underlying assumptions, including the bow glancing impact scenario, characterizing the contact area in FEA, such as load patch size, and the critical parameters related to ice conditions, including ice strength, such as $P_0$ and ex.

The two cases illustrate that collision energy and deformation depend on the ship's speed and ice conditions (thickness and mass) for a given ship and its structure. In general, the approach and corresponding look-up table(s) from this work enable a systematic mapping of the ship's structural capacities and limitations as a function of ice conditions and ship speed.

With such a mapping in hand, the actual conditions in which a vessel is operating at any point can be used to guide the ship's routing and speed to ensure it remains within an acceptable boundary, whether expressed in terms of collision energy, deformation, speed, route (to avoid specific ice conditions), or some combination of these. To do so in practice requires not just that the ship's limitations be known in advance, but that the prevailing ice conditions be sensed and that the resulting information be communicated effectively to the ship's operator(s). This last issue is the focus of the current work being undertaken by the first author.


## ACKNOWLEDGEMENTS

The financial support of the Natural Sciences and Engineering Research Council (NSERC) Alliance Grant is acknowledged with gratitude.

## REFERENCES


Canadian Coast Guard. (2022). *Ice Navigation in Canadian Waters*. Retrieved March 2025 from https://www.ccg-gcc.gc.ca/publications/icebreaking-deglacage/ice-navigation-glaces/page05-eng.html

Daley, C. (1999, May). Energy based ice collision forces. In *Proceedings of the 15th International Conference on Port and Ocean Engineering under Arctic Conditions (POAC)* (Vol. 2, pp. 674-686).

Daley, C., Hermanski, G., Pavic, M., & Hussein, A. (2007). Ultimate strength of frames and grillages subject to lateral loads–an experimental study. In *10th international symposium on practical design of ships and other floating structures (PRADS), Houston, Texas, United States of America*.

Daley, C., & Kim, H. (2010). Ice collision forces considering structural deformation. In *International Conference on Offshore Mechanics and Arctic Engineering*, January, **49125**, 817-825.

Daley, D., Dolny, J., & Daley, K. (2017). Safe Speed Assessment of DRDC Notional Destroyer in Ice, Phase 2 of Ice Capability Assessment.

Dolny, J., Yu, H. C., Daley, C., & Kendrick, A. (2013). Developing a technical methodology for the evaluation of safe operating speeds in various ice conditions. In *Proceedings of the International Conference on Port and Ocean Engineering Under Arctic Conditions*.

Ehlers, S., & Tabri, K. (2012). A combined numerical and semi-analytical collision damage assessment procedure. *Marine Structures*, **28** (1), 101-119.

Hallquist, J. O. (2006). LS-DYNA theory manual. *Livermore software Technology corporation*, *3*, 25-31.

IACS. (2010). Shipbuilding and Repair Quality Standard. International Association of Classification Societies.

IACS. (2019). Regulations concerning polar class. International Association of Classification Societies, London.

Lubbad, R., & Løset, S. (2011). A numerical model for real-time simulation of ship–ice interaction. *Cold Regions Science and Technology*, **65** (2), 111-127.

Minorsky, V. U. (1958). *An analysis of ship collisions with reference to protection of nuclear power plants* (No. NP-7475). Sharp (George G.) Inc., New York.

Pedersen, P. T. (1995). Collision and grounding mechanics. *Proceedings of WEMT*, **95** (1995), 125-157.

Popov, Y., Faddeyev, O., Kheisin, D., & Yalovlev, A. (1967). Strength of ships sailing in ice. *US Army Foreign Science and Technology Center (Translation)*.

Quinton, B. W. (2015). Experimental and numerical investigation of moving loads on hull structures. Doctoral dissertation, Memorial University of Newfoundland.

Zhang, S., Pedersen, P. T., & Villavicencio, R. (2020). Ship collision damages: Case studies. In *Developments in the Collision and Grounding of Ships and Offshore Structures,* London, March, 17-23.